

CONFIDENTIAL

Copy 5
RM E52B27

FOR REFERENCE

JUN 1 1957

C11

NOT TO BE TAKEN FROM ROOM

NACA

RESEARCH MEMORANDUM

AN EXPERIMENTAL CASCADE STUDY OF THE EFFECTS OF A SOLIDITY
REDUCTION ON THE TWO-DIMENSIONAL AERODYNAMIC
CHARACTERISTICS OF A TURBINE-ROTOR BLADE
SUITABLE FOR AIR COOLING

By Henry W. Plohr and William J. Nusbaum

CLASSIFICATION CHANGED
Propulsion Laboratory
Cleveland, Ohio

UNCLASSIFIED

To

By authority of

NACA Res abs
4RN-119

Date

effective
Aug. 16, 1957

AM 9-5-57

CLASSIFIED DOCUMENT

This material contains information affecting the National Defense of the United States within the meaning of the espionage laws, Title 18, U.S.C., Secs. 793 and 794, the transmission or revelation of which in any manner to an unauthorized person is prohibited by law.

NATIONAL ADVISORY COMMITTEE FOR AERONAUTICS

WASHINGTON
May 8, 1952

CONFIDENTIAL

NACA RM E52B27



NATIONAL ADVISORY COMMITTEE FOR AERONAUTICS

RESEARCH MEMORANDUM

AN EXPERIMENTAL CASCADE STUDY OF THE EFFECTS OF A SOLIDITY REDUCTION
ON THE TWO-DIMENSIONAL AERODYNAMIC CHARACTERISTICS OF
A TURBINE-ROTOR BLADE SUITABLE FOR AIR COOLING

By Henry W. Flohr and William J. Nusbaum

SUMMARY

An experimental two-dimensional investigation of the mechanism of the flow and the losses involved in the operation of a low-solidity highly loaded turbine-blade profile suitable for use in an air-cooled turbine has been made in a cascade. The nature of the flow in the channel formed by adjacent blades and at the exit of the blade row was investigated by static-pressure measurements and schlieren photographs over a wide range of pressure ratios. Flow conditions at the exit of the blade row were evaluated from the static-pressure measurements by the conservation-of-momentum principle. The results of this investigation were compared with similar published cascade data on the same blade profile at a higher solidity. The original design solidity of 1.38 was reduced to 1.06 for this investigation.

The total turning angle of the low-solidity configuration was less than that of the design-solidity configuration at all pressure ratios. This difference was greatest at low pressure ratios, because of the greater separation of the flow from the blade suction surface in the case of the low-solidity configuration. Maximum turning, 71.3° , was obtained when the blade first became fully loaded. At this point no separation was evident and the turning angle was 6° less than the maximum turning of the design-solidity configuration. The low-solidity configuration required a $7\frac{1}{2}$ percent higher pressure ratio in order to fully load the blade. At this point the maximum tangential component of the exit critical-velocity ratio was 5 percent below that of the design-solidity configuration. The two-dimensional losses of the low-solidity configuration were higher than those of the design-solidity configuration at low pressure ratios but were comparable or only slightly higher at pressure ratios high enough to fully load the blade. As the pressure ratio was increased from 1.56 to a value great enough to fully load the blade, the velocities on the suction surface of the low-solidity configuration increased on 80 percent of the blade suction surface, whereas for the design-solidity configuration only 40 percent of the suction surface had increased velocities.

INTRODUCTION

In the design of gas turbines having air-cooled blades for application to aircraft propulsion, the use of low-solidity blading is desirable in order to reduce the amount of coolant required, to reduce the turbine-wheel weight, and to simplify the mechanical design of the rotor. Low-solidity blading in turbines having high power output requires high blade loading which may introduce severe pressure losses due to flow separation and supersonic shock losses. Some indication of the turbine losses involved in the use of low-solidity blading can be obtained from two-dimensional cascade tests. While cascade tests will not indicate all of the turbine losses involved in the use of low-solidity blading, any losses found in the two-dimensional tests that can be attributed to the low solidity of the blading would also appear in the rotating unit. A comparison of cascade tests of a turbine blade profile at a low solidity with similar tests of the same profile at a higher solidity will give an indication of the additional two-dimensional profile losses involved in low-solidity operation.

The results of a two-dimensional cascade investigation of the mechanism of the flow and the losses involved in the operation of a blade configuration suitable for use in air-cooled turbines by virtue of its relatively low solidity and thick trailing edge profile are presented in reference 1. The results of this investigation indicated that supersonic velocities were obtained over the greater portion of the blade suction surface, which resulted in high blade loading without an appreciable decrease in efficiency from that obtained using blades with lower surface velocities.

The solidity of the blading configuration investigated in reference 1 was 1.38, representative of the lower values being used in current aircraft gas turbines. In order to determine the mechanism of the flow and the two-dimensional losses involved in the operation of this same profile at a reduced solidity, a two-dimensional cascade investigation of this profile at a solidity of 1.06 has been made at NACA Lewis Laboratory. The results of this investigation are reported herein and are compared with the results obtained in reference 1.

The mass-averaged velocity at the cascade exit, as determined from momentum considerations using blade and wall static-pressure taps, are presented herein along with schlieren photographs of the flow through the blade passages. The losses, as indicated by a velocity coefficient (defined as the ratio of the mass-averaged velocity to the isentropic velocity as measured at the cascade exit), are also presented.

The blade-surface velocity distribution at a low pressure ratio and at the point of maximum blade loading was also determined from the blade-surface static-pressure measurements assuming isentropic flow.

All the experimental studies were carried out for an inlet temperature of 600° R and an inlet pressure within 5 percent of 22.0 pounds per square inch. The static-pressure survey studies were made at total-to-static pressure ratios ranging from 1.47 to 2.86, whereas the schlieren studies were made for total-to-static pressure ratios from 1.53 to 3.11.

SYMBOLS

The following symbols are used in this report:

- g gravitational constant (32.2 ft/sec²)
- K frictional drag force (lb)
- m mass flow (slug/sec)
- P pressure force (lb)
- p pressure (lb/sq ft)
- R gas constant (ft-lb/(lb)(°R))
- T absolute total temperature (°R)
- W velocity relative to blade (ft/sec)
- W_{cr} critical speed of sound relative to blade, $\left(\sqrt{\frac{2\gamma}{\gamma + 1} gRT} \right)$
- B angle of flow measured from tangential direction (deg)
- γ ratio of specific heats, 1.40 for air

Subscripts:

- q pressure surface of blade downstream of station 2
- s suction surface of blade downstream of station 2
- u tangential component
- x axial component
- 1 inlet to cascade
- 2 station in blade passage (fig. 1)

3 station downstream of blade row where exit flow is evaluated

Superscripts:

' stagnation state

THEORETICAL ANALYSIS

Experimental Method for Obtaining Flow Conditions

at Cascade Exit

The flow conditions at the blade-row exit were evaluated experimentally by the conservation-of-momentum principle in the same manner as that presented in reference 1. The equations of momentum may be applied to the fluid enclosed by the area ABCDEFA shown in figure 1. The components of momentum are resolved in the axial and tangential directions to give the corresponding velocity components as follows:

$$W_{x,3} = W_{x,2} + \frac{P_2 + P_{x,s} - K_{x,s} - P_{x,q} - K_{x,q} - P_3}{m} \quad (1a)$$

$$W_{u,3} = \frac{P_{u,q} - K_{u,q} - P_{u,s} - K_{u,s}}{m} \quad (1b)$$

For the blade profile investigated, the velocity at station 2 was assumed to be in the axial direction. The magnitude of the mass-averaged velocity at station 2 and the velocity on the blade surfaces AF and BC can be determined from the static-pressure distribution assuming isentropic-flow relations. The mass flow was calculated at this station using the measured pressure distribution and isentropic-flow relations. A flow coefficient of 1 was assumed. The pressure forces P_2 , P_q , P_s , and P_3 can be determined experimentally by integrating the static-pressure distribution over the corresponding areas. The frictional forces K_s and K_q are comparatively small and can be calculated with sufficient accuracy by assuming the boundary layer to be turbulent from the leading edge and by using conventional relations for calculating the drag as in reference 2. The forces along the boundaries CD and EF are equal and opposite and therefore have no effect on the flow.

The mass-averaged velocity calculated from equation (1) is higher than the velocity of a uniform fluid stream having the same momentum. This difference can be considered to be the result of mixing losses that take place in a fluid stream with a velocity gradient as the fluid attains a uniform velocity.

APPARATUS

Blade Profile

The blade profile used in this investigation was the mean section of an air-cooled nontwisted rotor blade designed for a turbine that is applicable for use in contemporary turbojet engines and is shown in figure 2. This is the same blade profile that was investigated in reference 1 at a solidity of 1.38. The inlet-flow angle β_1 for all data presented was 53.8° measured from the tangential direction. This gave a critical-velocity ratio of 0.770 at the blade-row inlet for all total-to-static pressure ratios equal to and greater than 1.8. The guided channel formed by adjacent blades was slightly convergent from the blade-row entrance to exit. Because of the wide throat section at the guided-passage exit, this blade design was able to pass a high mass flow per unit of annulus area. The solidity of the blade configuration investigated was 1.060 based on the axial width of the blade (1.063 based on blade chord).

Equipment

The equipment used in this investigation is identical to that used in reference 1 except for the changes necessitated by the difference in solidity. For this investigation, two experimental test sections were made, one for making static-pressure surveys and another for obtaining schlieren photographs. The axial width of the blades used was 1.40 inches. Each test section had four blades and two end blocks forming five equal passages.

The static-pressure-survey test section had 22 static-pressure taps on the pressure surface and 28 taps on the suction surface of the blade in order to determine the velocity distribution of the profile. A total of 30 static-pressure taps on the blade profile downstream of station 2, 18 wall taps across the channel located at station 2, and 33 wall taps spaced approximately $\frac{1}{10}$ inch apart located at station 3, which was 0.59 inch downstream of the blade row, were used to determine the pressure distribution at these stations in order to calculate the velocity at the exit of the blade row by the conservation-of-momentum principle (fig. 2). The static-pressure distribution at station 3 was used for determining the average pressure at the exit of the cascade in order to compute the total-to-static pressure ratio across the blade row. All the experimental static pressures were determined from the center passage of the cascade where the flow uniformity most nearly simulated an infinite cascade. A total of 13 wall static-pressure taps evenly spaced across the width of the cascade at the inlet to the blade row were used to

measure the static pressure at that point. A compartmented suction slot $1\frac{3}{8}$ inches upstream of the cascade was used for boundary-layer removal. The amount of air drawn through each compartment was adjusted until the static-pressure distribution at the inlet to the blade row was uniform.

For the optical test section, the blades were held in place by pins fastened to four steel bars that were inlaid in the glass plates.

The inlet total pressure and total temperature were measured in the surge tank just upstream of the cascade. The inlet total temperature was measured with a thermocouple and read on a potentiometer to within 3° F. The static pressures were read to an accuracy within 0.05 pound per square inch. The static pressure at a point in the ducting downstream of the test section was observed for both the static-pressure surveys and the optical tests in order to correlate the schlieren photographs with pressure-survey data.

Additional information about the experimental equipment in which the test section was installed is given in reference 2.

RESULTS AND DISCUSSION

The exit-flow velocity, angle, and velocity coefficient, as determined from the static-pressure surveys, are shown in figure 3. The exit-flow velocity components relative to the blade are presented in terms of a critical-velocity ratio, defined as the ratio of the experimentally determined mass-averaged velocity component to the critical speed of sound (W_{cr}). Similar results taken from reference 1 for the design-solidity configuration are also shown in figure 3 for purposes of comparison. Schlieren photographs of the flow through the blade passages are shown in figure 4. All conclusions drawn from the schlieren studies were made by observing the flow through the center passage of the cascade (the third passage from the bottom of the photographs shown in fig. 4) since the flow through this passage most nearly simulated the flow through a passage of a cascade having an infinite number of blades.

The general phenomenon of the flow past the cascade of blades investigated in this report was similar to that of the design-solidity configuration reported in reference 1. At low pressure ratios, separation of the flow from the suction surface of the blade profile caused the flow to underturn from the minimum value of the exit-flow angle, which was obtained at the lowest pressure ratio for which the blade was fully loaded (where the tangential component of the exit critical-velocity ratio

$\left(\frac{W_u}{W_{cr}/3}\right)$ reached a maximum value). As the pressure ratio was increased from its lowest value, the region of separated flow was decreased until no separation was evident when maximum blade loading was obtained. As the pressure ratio was increased beyond the point where maximum blade loading was first obtained, the decrease in the downstream pressure only resulted in increasing the axial component of the exit critical-velocity ratio and the downstream shock losses.

Although the general flow phenomena for the two solidities are similar, quantitative differences were found. At corresponding pressure ratios, the low-solidity cascade has a lower exit tangential critical-velocity ratio and a higher axial critical-velocity ratio than the design-solidity configuration (fig. 3). This is reflected in a consistently higher exit-flow angle (lower turning angle) for the low-solidity configuration. The difference in the turning angle of the two solidities is greater at low pressure ratios, because the separation of the flow from the blade suction surface of the low-solidity configuration was more severe. In figure 4(a) the flow can be seen to separate from the midchord station to form a wide wake region. As the pressure ratio is increased, the chordwise position where separation starts moves towards the trailing edge (fig. 4(b)). The photograph shown in figure 4(c), taken at a pressure ratio slightly above the point where maximum blade loading is first attained, is representative of the flow pattern at the pressure ratio where maximum blade loading is first obtained. The center passage, corresponding to the instrumented passage in the pressure survey tests, is free of severe separation. This attached flow is not obtained until the blade becomes fully loaded, and remains attached at all higher pressure ratios (fig. 4(d)).

A comparison of the blade-surface velocity distributions for both solidities at a total-to-static pressure ratio of 1.56 is shown in figure 5(a), and the velocity distributions at maximum blade loading are shown in figure 5(b). The data for the design-solidity configuration shown in figure 5(b) was taken from reference 1, whereas that shown in figure 5(a) was taken from unpublished data. The blade-surface velocities were calculated from the measured blade-surface static pressures assuming isentropic flow. In the channel formed by adjacent blades, the departure from this condition is small when the blade is fully loaded, as is apparent in the schlieren photographs of figure 4(d) of this report and figure 4(e) of reference 1. For the data shown in figure 5(a), which was taken at a pressure ratio of 1.56, this assumption is valid on that portion of the blade where separation does not take place. Figure 4(a) indicates that separation takes place at about the 50-percent chord station of the low-solidity configuration, whereas figure 4(b) of reference 1 indicates that the design-solidity configuration separates at the 70-percent chord station. Therefore, the isentropic velocities shown in figure 5(a) are higher than the actual velocities over the corresponding separated flow regions on the blade surface.

A comparison of figure 5(a) with figure 5(b) indicates the change in the blade-surface velocities that occurs as the total-to-static pressure ratio is increased from a value of 1.56 to the value required to fully load the blade. Because the design-solidity configuration chokes at the exit of the guided passage at a total-to-static pressure ratio slightly greater than 1.56, that portion of the blade suction surface downstream of the guided channel is the only portion of the blade surface on which the velocities change with increasing pressure ratio. The low-solidity configuration, which chokes at a pressure ratio of 1.80, has an entirely different velocity distribution as the pressure ratio is increased to the point of maximum blade loading. The velocity on the suction surface increases over the whole surface, reaching a peak critical-velocity ratio of 1.63.

The velocity distributions shown in figure 5 indicate that high velocities are obtained near the leading edge of the profile for both configurations. At low pressure ratios the downstream pressure is too high to support these high velocities all the way to the blade trailing edge, and as a consequence, the fluid velocity decreases and the pressure rises along the blade suction surface causing flow separation. Figure 5(a) indicates that 80 percent of the blade suction surface for the low-solidity configuration, and 40 percent of the blade suction surface for the design-solidity configuration has a decreasing velocity gradient. At maximum blade loading where the pressure ratio is greater (fig. 5(b)) the downstream pressure is low enough to support high velocities on the suction surface and thus presents a more favorable pressure gradient to the boundary layer.

If high velocities could be avoided on the blade suction surface near the blade leading edge, subsequent velocity decreases and flow separation might be avoided. These high leading edge velocities could be avoided by increasing the inlet flow angle β_1 .

The low-solidity configuration becomes fully loaded at a pressure ratio of about 2.0, where the exit tangential critical-velocity ratio reaches a maximum value of 0.61 (fig. 3). This value is about 5 percent below the maximum exit tangential critical-velocity ratio obtained for the design-solidity configuration and is not obtained until the pressure ratio is about $7\frac{1}{2}$ percent higher. At about the same pressure ratio, the exit-flow angle β_3 reaches a minimum value of 54.9° for a total turning angle of 71.3° . This is 6° less than the maximum total turning angle obtained in reference 1.

The velocity coefficient (defined as the ratio of the mass-averaged velocity to the isentropic velocity at the cascade exit, station 3) of the two solidities is shown in figure 3. This velocity coefficient does not include the mixing losses that would take place in the fluid if it were allowed to come to a uniform velocity without loss of momentum.

2Q

Since the mixing losses are highest when the velocity distribution at station 3 has the greatest variation, the difference between the measured velocity coefficient and one that would include mixing losses would increase with increasing pressure ratio and would probably be greatest for the low-solidity cascade. An estimate of the mixing loss was made for the low-solidity profile at a pressure ratio just below that required to fully load the blade. For this condition the velocity coefficient was found to be lowered by 2 to 3 percent.

2415

At low pressure ratios, the greater separation encountered in the low-solidity design reduced the velocity coefficient below that of the design-solidity configuration. As the pressure ratio is increased from the lowest value, the difference between the velocity coefficient of the two solidities becomes less because of the reduced separation losses encountered in the low-solidity design. At a pressure ratio of 1.9 and above, the velocity coefficient of the low-solidity cascade is above that of the design-solidity cascade. If the mixing losses were taken into account, the velocity coefficient of the low-solidity cascade would probably be comparable or slightly less than that of the design-solidity cascade for the complete range of pressure ratios. From the velocity-coefficient data, the losses of the low-solidity cascade are concluded to be greater than those of the design-solidity cascade at low pressure ratios but are comparable or only slightly higher when the pressure ratio is high enough to fully load the blade.

SUMMARY OF RESULTS

The results of an experimental two-dimensional cascade investigation of a low-solidity highly loaded turbine-blade profile suitable for use in an air-cooled turbine were compared with similar published cascade data on the same blade profile at a higher solidity. The original design solidity of 1.38 was reduced to 1.06 for this investigation. The results of the two investigations yielded the following comparison:

1. The turning angle of the low-solidity configuration was less than that of the design-solidity configuration at all pressure ratios. The difference in the turning angle was greatest at low pressure ratios, because of the greater separation of the flow from the blade suction surface in the case of the low-solidity configuration. At the pressure ratio where the blade first became fully loaded (where the tangential component of the exit critical-velocity ratio $\left(\frac{W_{u1}}{W_{cr}}\right)_3$ reached a maximum value) and the turning angle was the greatest, no severe separation was noticed. The total turning angle at this point was 71.3° , 6° less than the maximum turning of the design-solidity configuration.

2. The low-solidity configuration became fully loaded at a pressure ratio of about 2.0, $7\frac{1}{2}$ percent higher than the pressure ratio at which the design-solidity configuration became fully loaded. The maximum tangential component of exit critical-velocity ratio was 0.61, 5 percent below the value obtained with the design-solidity configuration.

3. The two-dimensional losses of the low-solidity configuration were higher than those of the design-solidity configuration at low pressure ratios but were comparable or only slightly higher at pressure ratios high enough to fully load the blade.

4. As the total-to-static pressure ratio across the blade row was increased from 1.56 to a value great enough to fully load the blade, the velocities on the suction surface of the low-solidity configuration increased on 80 percent of the blade surface, whereas for the design-solidity configuration, only 40 percent of the suction surface had increased velocities. The suction-surface velocities for the low-solidity configuration reached a peak critical-velocity ratio of 1.63.

Lewis Flight Propulsion Laboratory
National Advisory Committee for Aeronautics
Cleveland, Ohio

REFERENCES

1. Plohr, Henry W., and Hauser, Cavour H.: A Two-Dimensional Cascade Study of the Aerodynamic Characteristics of a Turbine-Rotor Blade Suitable for Air Cooling. NACA RM E51G18, 1951.
2. Hauser, Cavour H., and Plohr, Henry W.: Two-Dimensional Cascade Investigation of the Maximum Exit Tangential Velocity Component and Other Flow Conditions at the Exit of Several Turbine Blade Designs at Supercritical Pressure Ratios. NACA RM E51F12, 1951.

2413

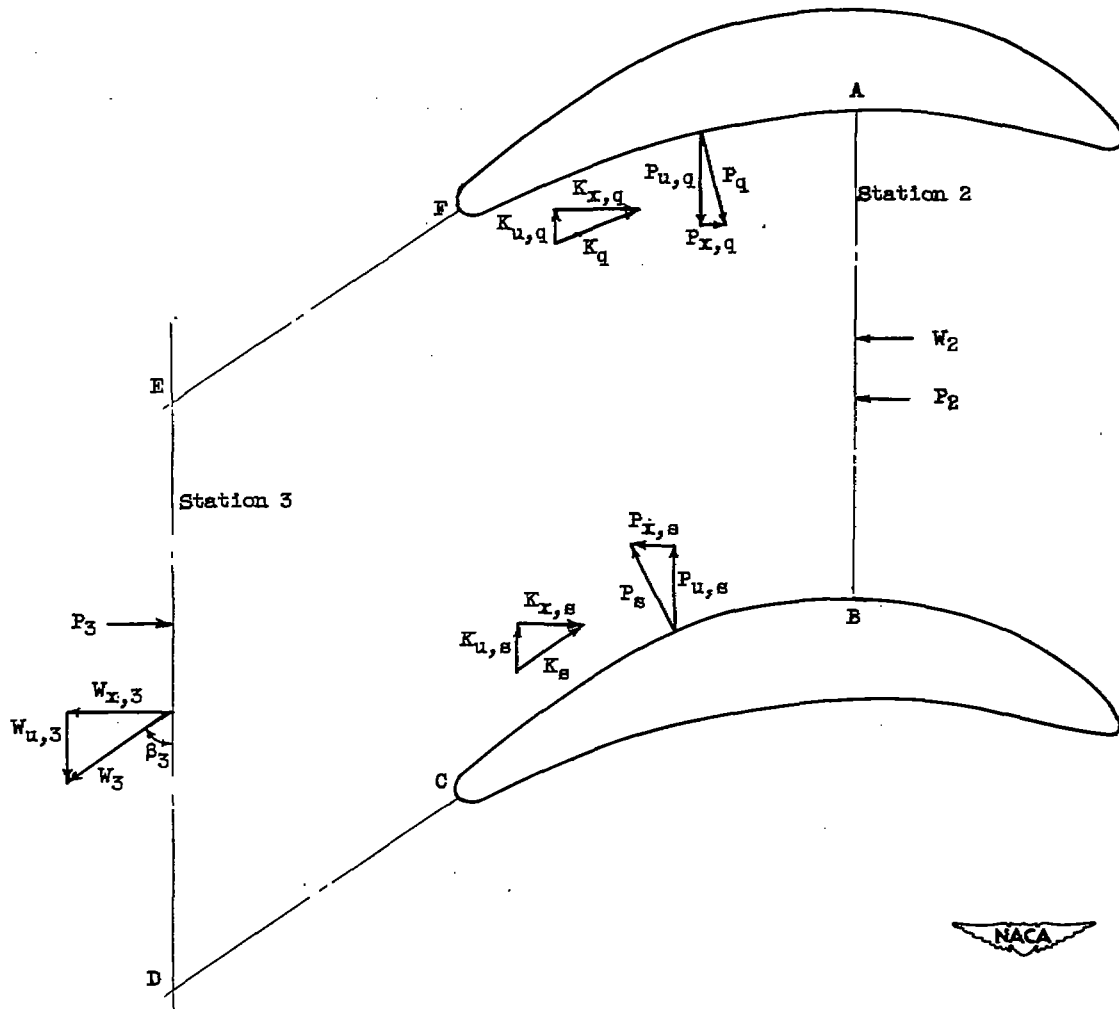
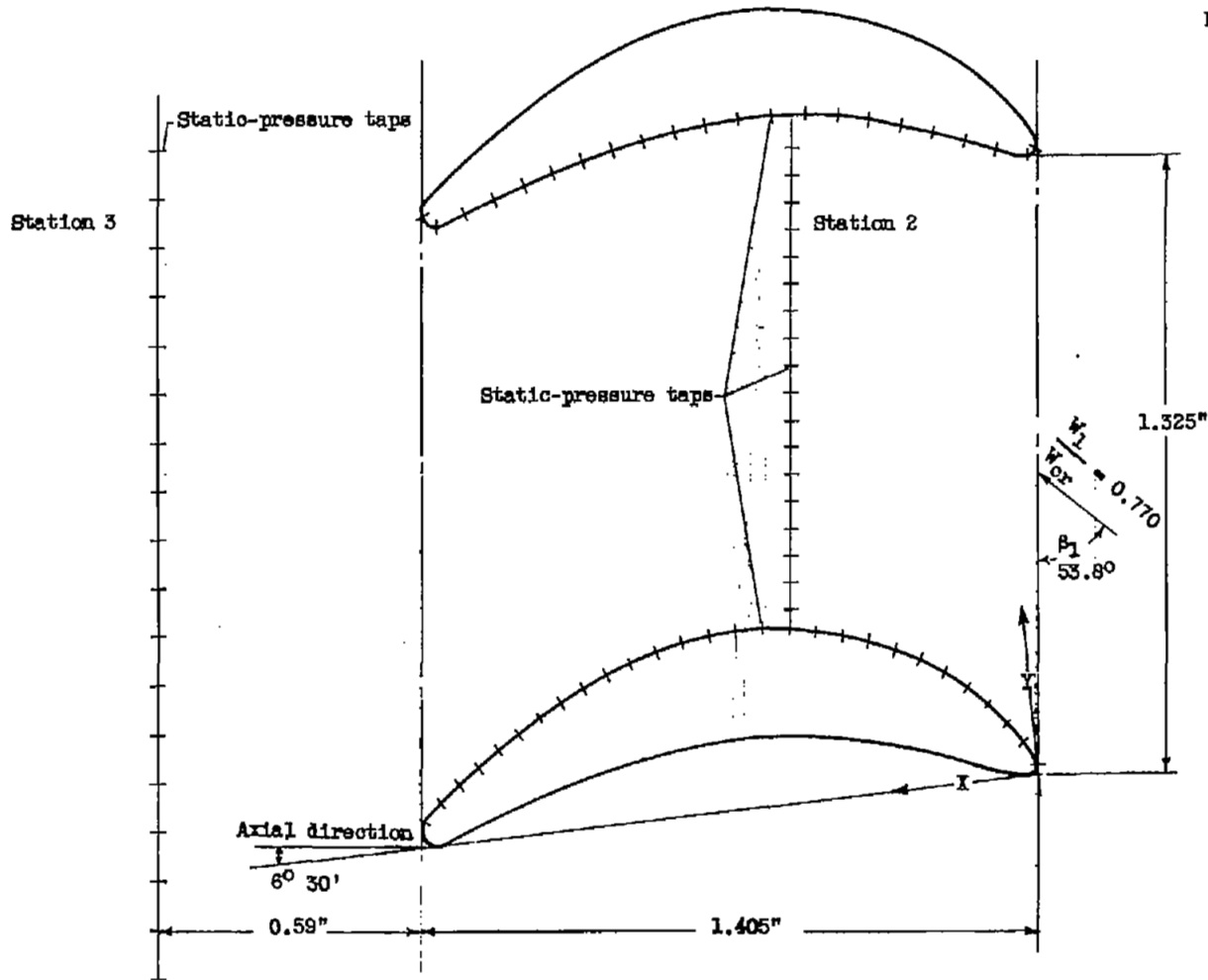


Figure 1. - Diagram of cascade-flow conditions measured in static-pressure surveys for evaluation of exit flow by conservation-of-momentum principle.



Blade profile coordinates

X	Y	
	Suction surface	Pressure surface
0	0.022	0.022
.033	.088	.002
.145	.209	.040
.383	.337	.119
.621	.384	.150
.859	.355	.138
1.097	.259	.095
1.336	.112	.010
1.583	.077	0
1.412	.057	.037



Figure 2. - Blade profile showing location of static-pressure taps.

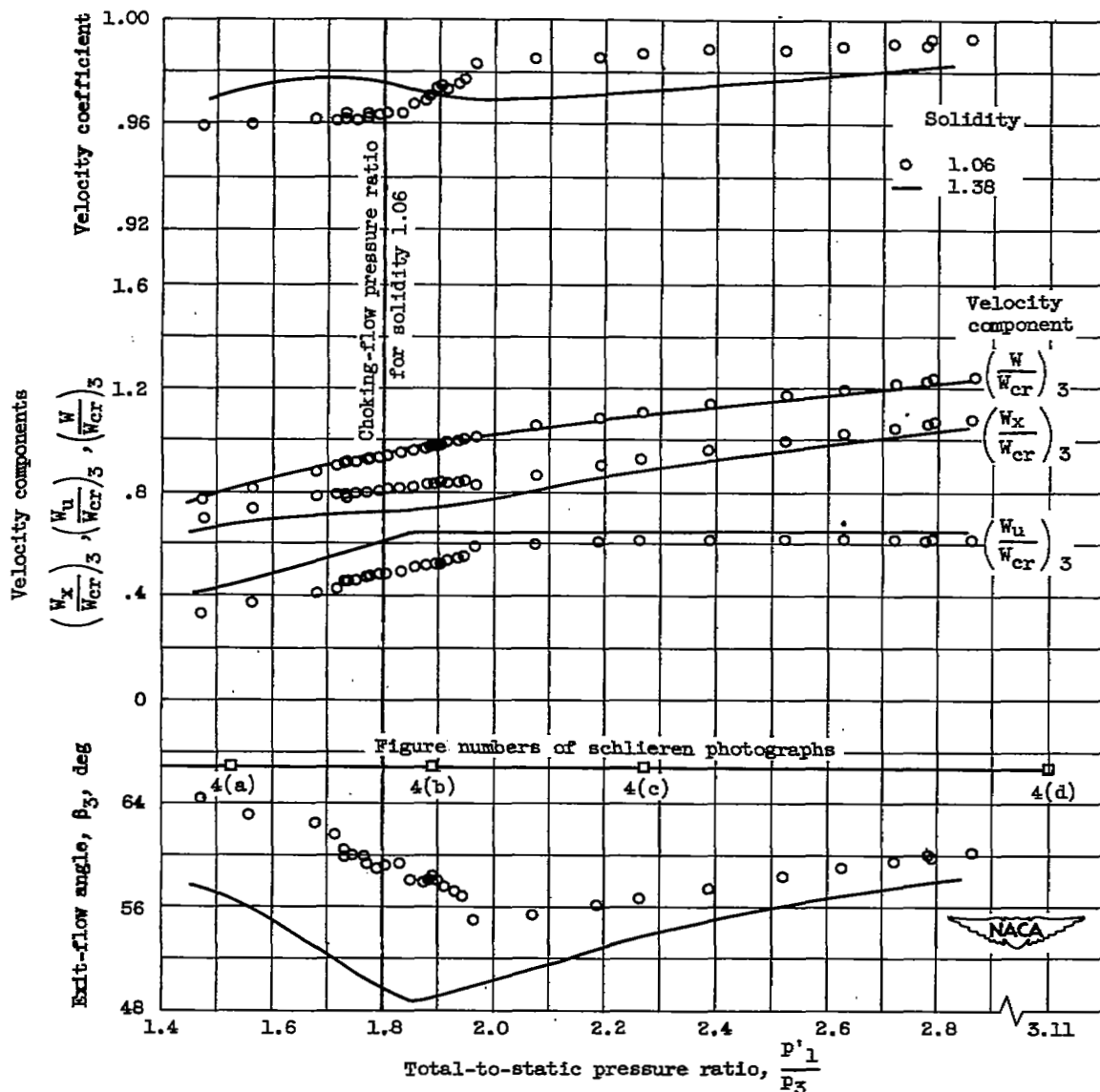
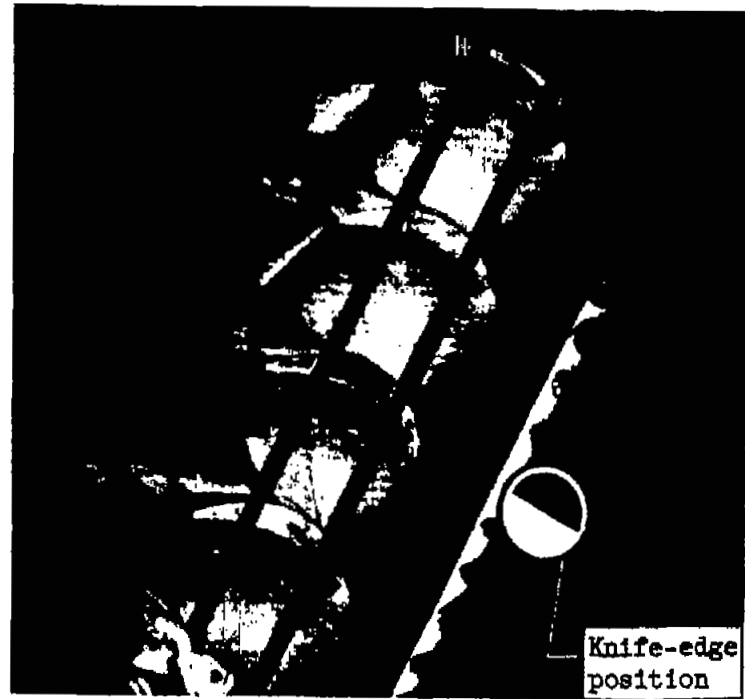


Figure 3. - Flow conditions at cascade exit (station 3) as determined from static-pressure surveys.

2413



(a) Total-to-static pressure ratio, 1.53.

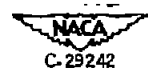
C-29241

(b) Total-to-static pressure ratio, 1.89.

Figure 4. - Schlieren studies of flow through cascade.

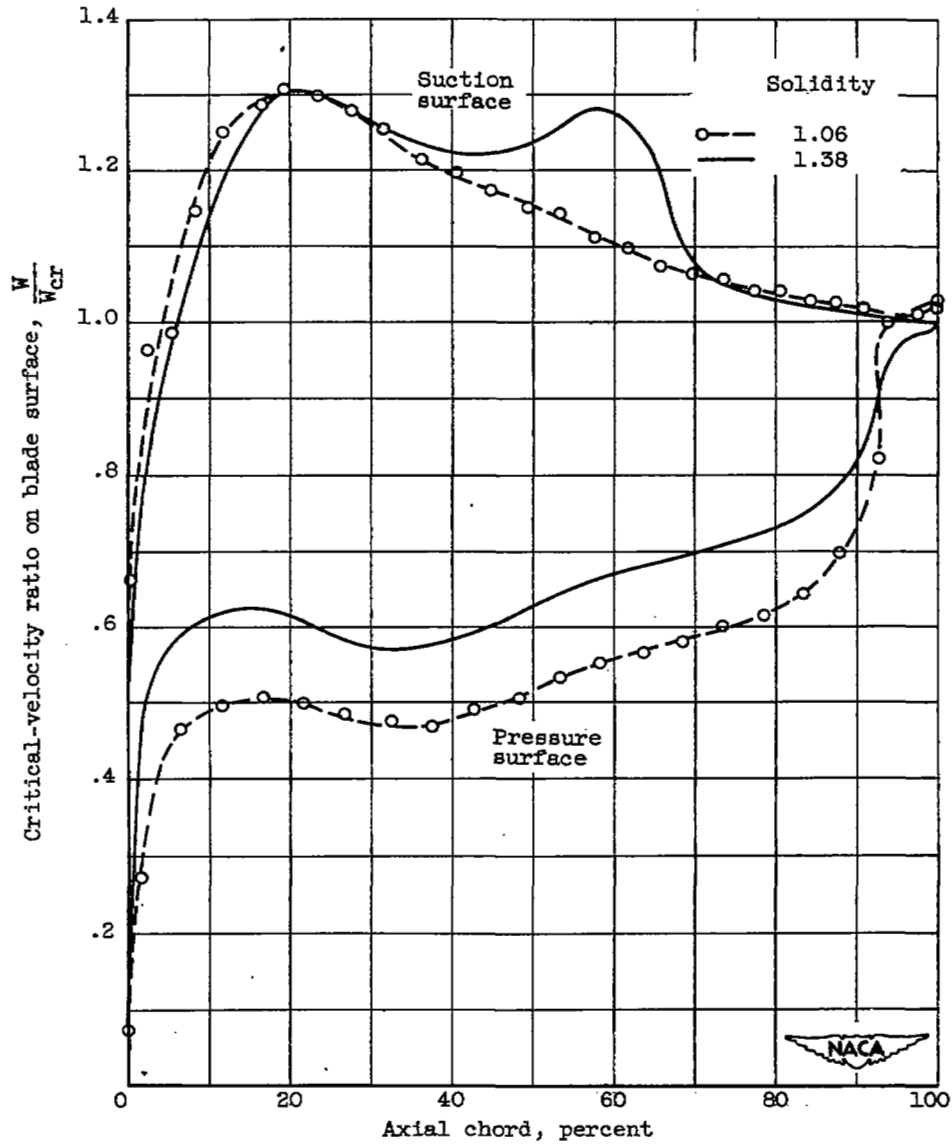


(c) Total-to-static pressure ratio, 2.27.



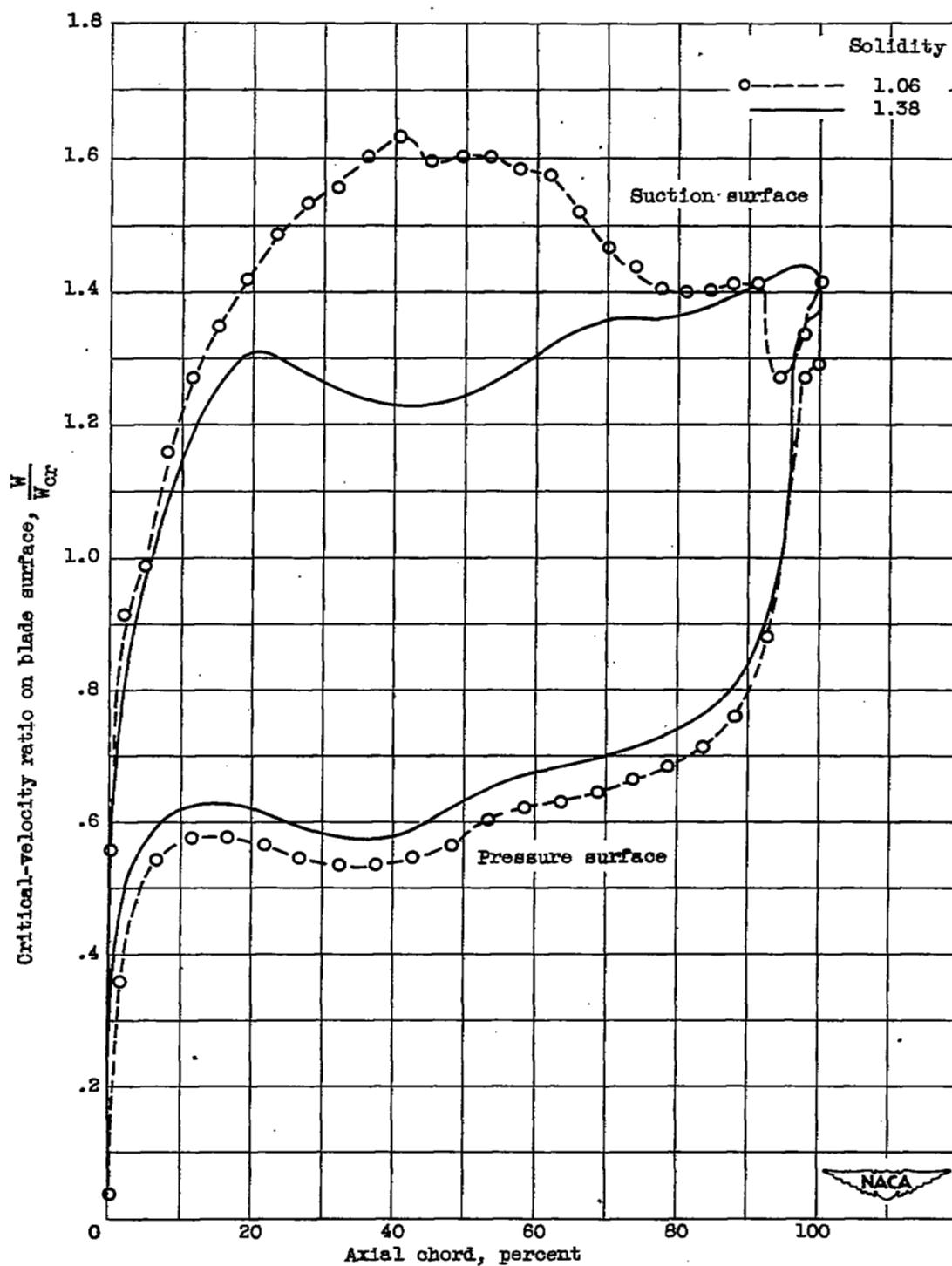
(d) Total-to-static pressure ratio, 3.11.

Figure 4. - Concluded. Schlieren studies of flow through cascade.



(a) At a total-to-static pressure ratio of 1.56.

Figure 5. - Blade-surface velocity distribution.



(b) At maximum blade loading.

Figure 5. - Concluded. Blade-surface velocity distribution.

SECURITY INFORMATION

NASA Technical Library



3 1176 01436 0029

